Available online at www.sciencedirect.com
SCIENCE DIRECT®
Journal of Power Sources 140 (2005) 340–345
JOURNAL OF POWER SOURCES
www.elsevier.com/locate/jpowsour

Short communication

Long-term thermal cycling of Phlogopite mica-based compressive seals for solid oxide fuel cells

Yeong-Shyung Chou*, Jeffry W. Stevenson

K2-44, Materials Department, Pacific Northwest National Laboratory, 902 Battelle Boulevard, P.O. Box 999, Richland, WA 99352, USA

Received 6 August 2004; accepted 26 August 2004
Available online 13 October 2004

Abstract

Planar solid oxide fuel cells (SOFCs) require sealants to function properly in harsh environments at elevated temperatures. The SOFC stacks are expected to experience multiple thermal cycles (perhaps thousands of cycles for some applications) during their lifetime service in stationary or transportation applications. As a result, thermal cycle stability is considered a top priority for SOFC sealant development. In previous work, we have developed a hybrid mica-based compressive seal with very low leak rates of 2–4 $\times$ 10^{-2} to 10^{-3} sccm cm^{-1} at 800 °C, and showed stable leak rates over limited thermal cycles. In this paper we present results of long-term thermal cycle testing (>1000 thermal cycles) of Phlogopite mica-based compressive seals. Open-circuit voltage (OCV) was measured on a 2 in. $\times$ 2 in. 8-YSZ plate with the hybrid Phlogopite mica seals during thermal cycling in a dual environment (2.75% H_2/Ar versus air). During two long-term cycling tests, the measured OCVs were found to be consistent with the calculated Nernst voltages. The hybrid mica seal showed excellent thermal cycle stability over 1000 thermal cycles and can be considered a strong candidate for SOFC applications.

Keywords: Open-circuit voltage; Phlogopite mica; Solid oxide fuel cell; Leak rates; Thermal cycle

1. Introduction

Planar solid oxide fuel cells require a special sealant or sealants in order to function properly at elevated temperatures in the SOFC environment, which involves exposure to both oxidizing (air) and reducing (fuel) atmospheres. The sealant needs to provide zero or low leak rates to avoid direct mixing of the fuel and oxidant gases or leakage of fuel gas from the stack. It has to demonstrate long-term thermal and chemical stability in the SOFC environments (5000 h or more). Finally, it has to survive multiple thermal cycles (possibly thousands of cycles for some applications) during lifetime service in stationary or transportation applications. To do so, it has to be able to withstand transient stresses developed during startup or shutdown, and residual stresses due to mismatch in thermal expansion of different SOFC stack components. Currently, there are three primary approaches for SOFC seal development: rigid glass (or glass-ceramics and glass fiber composite) seals [1–5], metallic brazes [6,7], and compressive seals [8–12]. Among these studies, none has investigated the long-term thermal cycle stability (i.e., hundreds of cycles or more). As the thermal cycle stability appears to be a top priority for SOFC seal development, this paper reports the results of long-term thermal cycle testing of compressive mica seals. This study is a continuation of previous work on the "hybrid" mica compressive seal which has exhibited very low leak rates compared to conventional mica gasket seals [6], and also demonstrated thermal cycle stability over a limited number of thermal cycles. In this paper, we present results for two long-term thermal cycle stabilities of two "hybrid" mica seals. Open-circuit voltage (OCV) was used to characterize the thermal cycle stability of these mica seals using a standard 8-YSZ electrolyte plate. In addition, leak rates were measured and compared to the estimates calculated from OCVs.

* Corresponding author. Tel.: +1 509 375 2527; fax: +1 509 375 2186.
E-mail address: yeong-shyung.chou@pnl.gov (Y.-S. Chou).

0378-7753/$ – see front matter © 2004 Elsevier B.V. All rights reserved.
doi:10.1016/j.jpowsour.2004.08.030

2. Experimental

2.1. Materials and processing

The mica used in this study is a commercially available Phlogopite mica paper (McMaster-Carr, Atlanta, GA). The mica paper is composed of discrete mica flakes overlapping with each other [12]. The thickness is about 0.004 in. and the paper contains 3–5% of organic binders. In this study, two "hybrid" mica seals (i.e., mica paper sandwiched between two glass layers [8]) were tested for long-term thermal cycle stability. The glass layers were made by tape casting of a Ba–Al silicate glass developed at PNNL for SOFC sealing applications. The cast glass tapes had a thickness of about 0.015–0.020 in. after drying. The compressive stresses applied to the seals were 100 psi (sample #1) and 50 psi (sample #2). The compressive load was applied using a pneumatic cylinder and compressed air.

2.2. Open-circuit voltage test

In order to assess the sealing capability of the seals, OCV tests were conducted using 2 in. × 2 in. dense 8-YSZ plates prepared by slip casting 8-YSZ powders (TOSOH, Zirconia, TZ-8Y, Japan), followed by sintering at 1450 °C for 2 h. The sintered plates were machined to the desired size (2 in. × 2 in.) and thickness (∼1–2 mm), and then screen-printed with silver paste on both sides. After electrode sintering, Pt wire leads were connected for the OCV tests. A dense 8-YSZ plate was pressed between an Inconel600 top cap (2 in. ×2 in. with a wall thickness of 0.2 in.) and an alumina bottom support. The hybrid mica seals were placed between the 8-YSZ plate and the Inconel600 fixture. A schematic drawing of the OCV test fixture and the mica seal arrangement is shown in Fig. 1. The OCV measurements were conducted at 800 °C after dwelling at temperature for about 1.5–2 h. A low-hydrogen content gas (2.55–2.71% H_2/balance Ar with ∼3% H_2O) was used as the fuel with variable flow rates. Air was used as the oxidant on the cathode side with a flow rate of 100–200 sccm (standard cubic centimeter per minute). The samples were first fired slowly to 600 °C for binder burnout, followed by heating to 850 °C for 1 h and then cooling to the test temperature (800 °C) for 2 h. After the first dwell at 800 °C for 2 h, the samples were furnace cooled to 100 °C to initiate thermal cycling. The temperature profiles for the thermal cycling are shown in Fig. 2 for sample #2 (pressed at 50 psi). Sample #1 (pressed at 100 psi) was cycled with a different profile, i.e., rapid heating from 100 to 800 °C in

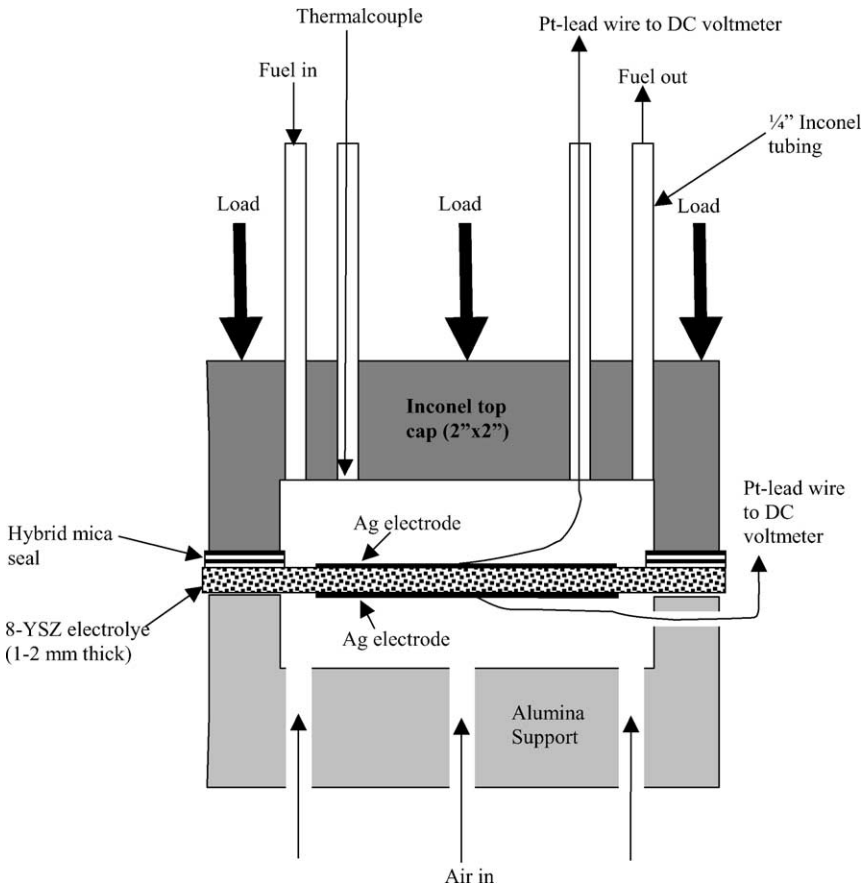

Fig. 1. Schematic showing the open-circuit voltage test fixture (2 in. × 2 in.) of dense 8-YSZ plate with compressive mica seals on the fuel side. The pressing cap was made of Inconel600 with four 1/4 in. Inconel600 tubes. The 8-YSZ plate was supported on an alumina block with three bottom holes for airflow.

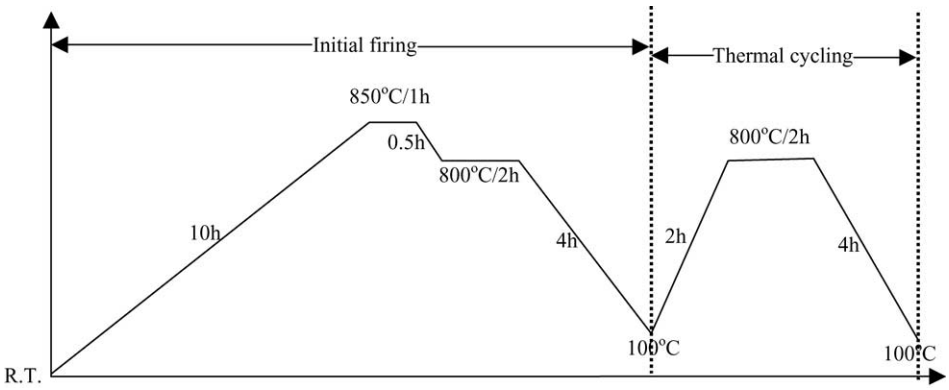

Fig. 2. Typical temperature profile for initial heat treatment and subsequent thermal cycling of seal sample #2 (50 psi). Sample #1 (100 psi) was heated more rapidly (100–800 °C in 35 min) and cooled slowly (in 5.5 h to 100 °C) during the thermal cycling period.

35 min, dwelling at 800 °C for 2 h, and cooling to 100 °C in 5 h and 25 min. Each thermal cycle took about 8 h, allowing three cycles to be conducted each day.

3. Results and discussion

3.1. Choice of low-hydrogen fuel for OCV and thermal cycle tests

A low-hydrogen fuel (2.55–2.71% H_2/balance Ar) was chosen for the long-term OCV and thermal cycling tests. The use of a dilute hydrogen fuel allowed for establishment of reducing conditions typical of the anode side of an SOFC with no risk of fire or explosion during the seal tests. The equilibrium oxygen partial pressure at 800 °C was calculated to be 6.45×10^{-19} atm for a 2.71% H_2/Ar fuel (with 3% H_2O), 1.68×10^{-21} atm for a 50% hydrogen fuel (with 3% H_2O), and 4.2×10^{-22} atm for pure moist hydrogen fuel (97% H_2/3% H_2O). It is evident that the use of a low-hydrogen fuel still provided a very reducing environment. The theoretical (Nernst) voltage for the dilute hydrogen fuel versus air across the 8-YSZ electrolyte is 0.934 V.

Another advantage of dilute hydrogen was an increased sensitivity to leaks during the OCV tests. During testing, a mica seal was applied only on the anode side of the YSZ plate, and then compressed with the Inconel600 fixture. The cathode side of the YSZ plate was directly pressed against the alumina support block without any seals in-between. The alumina support block had several holes underneath for airflow. The gas pressure at the anode side was maintained slightly higher than the ambient (∼0.2 psig) by using a downstream gas bubbler filled with ∼5 in. of water. Any leaked fuel would have minimum effect on the cathode side since it would immediately react with the air in the furnace chamber. On the other hand, any air (21% O_2) leaks into the anode chamber should have a more pronounced effect on the equilibrium oxygen partial pressure for a low-hydrogen (e.g., 2.71% H_2/Ar) fuel compared to a pure hydrogen fuel (e.g., 100% H_2).

3.2. Long-term OCV and thermal cycling of hybrid mica seal pressed at 100 psi

In the OCV tests, the fuel flow rate was fixed at 63 sccm. This flow rate would correspond to an 80% fuel utilization for a cell with an active area of 10 cm^2 operating at a current density of 0.75 A cm^{-2} on pure hydrogen (i.e., 97% H_2 + ∼3% H_2O). The OCV versus number of thermal cycles for the 2 in. × 2 in. 8-YSZ electrolyte plate with the hybrid Phlogopite mica-paper seal (sample #1) pressed at 100 psi is shown in Fig. 3. This sample survived 1000 thermal cycles when thermally cycled between 100 and 800 °C at a rapid heating rate of 20 °C min^{-1}. The initial (the first time reaching 800 °C) OCV was 0.934 V, exactly matching with the theoretical (Nernst) voltage for 2.71% H_2/balance Ar with 3% H_2O versus air at 800 °C. As the thermal cycles continued, the OCV decreased to about 0.92 V in the initial ∼50 thermal cycles (Fig. 3B) after which the OCV stabilized for the subsequent thermal cycles at 0.919 V ± 2 mV, which is only 1.7% lower than the Nernst voltage. The drop of OCV in the initial thermal cycles (Fig. 3B) is likely due to mica fracture (cleavage) associated with these cycles [11]. For hybrid mica seals, the glass interlayers will bond strongly to the mating materials (Inconel600 and 8-YSZ in the present study) and to the top several layers of the mica. During initial thermal cycling, the large CTE mismatch between the Inconel600 fixture (∼17 ppm $°C^{-1}$), the mica paper (∼11 ppm $°C^{-1}$), and the 8-YSZ electrolyte plate (∼10.5–11 ppm $°C^{-1}$) may form new fractures (leak paths) between the mechanically interlocked flakes in the mica paper. Fortunately, after a few dozen thermal cycles, the formation of additional leak paths apparently ceased, as the OCV remained fairly constant. Overall, the hybrid seals demonstrated the desired long-term thermal cycle stability.

3.3. Long-term OCV and thermal cycling of hybrid mica seal pressed at 50 psi

An identical hybrid Phlogopite mica seal (sample #2) was also tested for long-term thermal cycle stability at a lower

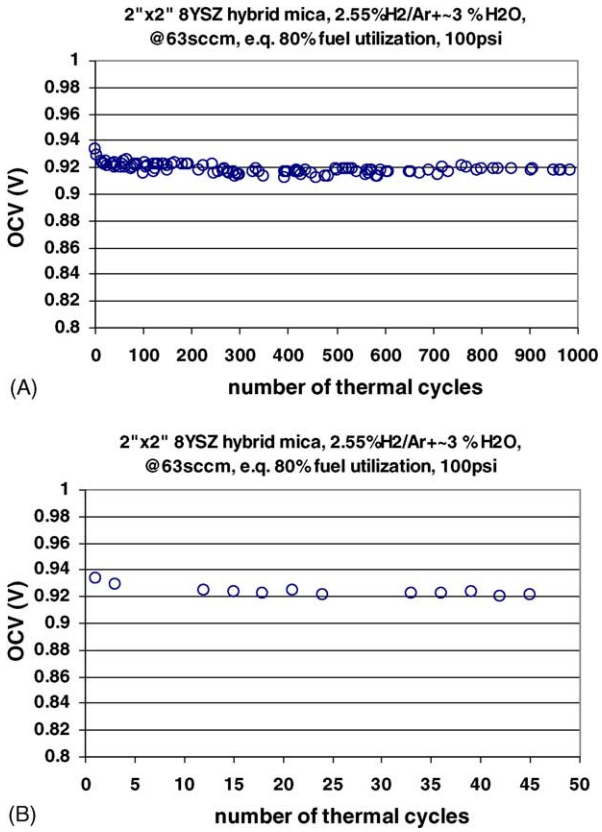

Fig. 3. OCV vs. thermal cycles of 2 in. × 2 in. 8-YSZ with hybrid mica seal pressed at 100 psi: (A) OCV over the whole range of thermal cycles and (B) OCV of the initial 50 thermal cycles. The fuel was 2.71% H_2/Ar + ∼3% H_2O at a flow rate of 63 sccm, equivalent to 80% fuel utilization by a cell of 10 cm^2 operating at a current density of 0.75 W cm^{-2}.

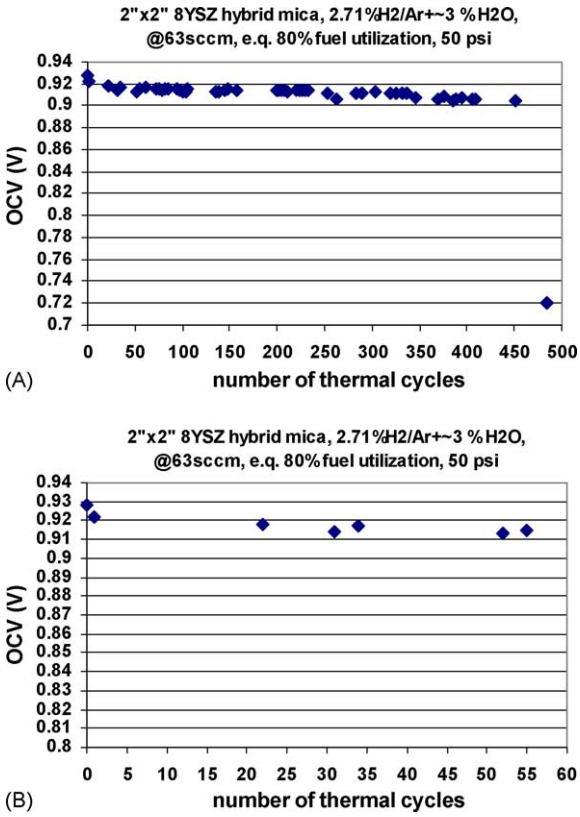

Fig. 4. OCV vs. thermal cycles of 2 in. × 2 in. 8-YSZ with hybrid mica seals pressed at 50 psi: (A) OCV over the whole range of cycles and (B) OCV of the initial 60 thermal cycles. The fuel was 2.71% H_2/Ar + ∼3% H_2O at a flow rate of 63 sccm, equivalent to 80% fuel utilization by a cell of 10 cm^2 operating at a current density of 0.75 W cm^{-2}.

applied compressive stress of 50 psi. Low compressive stress requirements are desired for actual SOFC stack seals to prevent the total compressive loads on the stack from being too high to be practical. The results of the measured OCV versus number of thermal cycles are shown in Fig. 4. The initial OCV was 0.928 V, about 6 mV lower than the Nernst voltage (0.934 V). The seal showed similar thermal cycle stability to sample #1 in that most of the OCV drop occurred in the initial ∼50 cycles (Fig. 4B), but different behavior in that the OCV continued to gradually drop to 0.906 V after 450 cycles. The 8-YSZ plate fractured at cycle #484, and the OCV dropped to 0.72 V due to mixing of air and fuel through the fracture. Considering the low concentration of H_2 in the fuel (2.71%), the effect of fuel leaking into air on the oxygen partial pressure on the cathode side should be small. For the case of air leaking into the anode side, one can calculate the equilibrium oxygen partial pressure at the anode side to be 5.76×10^{-15} atm (for an OCV = 0.72 V at 800 °C). This corresponds to an air leak rate of 3.87 sccm into the anode side or a normalized leak rate of 1.9–3.9 sccm cm^{-1} (the fracture length was found to be 1–2 cm). This simple calculation illustrates that the leak rates through cracks in conventional rigid glass seals could be 100 times higher than leak rates through hybrid mica seals. Also, such cracks yield highly localized leaks at which a hot-spot may form and ultimately lead to entire stack failure. Unlike the case for rigid glass seals, the leak through mica seals should be evenly distributed since there is a continuous network of voids between the discrete mica flakes. As a result, a hot-spot may not form, and total stack failure could be avoided even at higher leak rates.

3.4. Leak path in hybrid mica seals

It is important to point that the fuel was maintained at a slightly higher pressure (∼0.2 psi) than the surrounding air and the cathode side air. One would expect that the leak path would be one-way, i.e., fuel leakage from the anode side through the mica seal to the surrounding air, and that the measured OCV would be the same as the Nernst voltage if there was no fracture in the YSZ electrolyte since the cathode side was largely shielded from hydrogen leaks by the alumina support (Fig. 1). That is, leaking dilute hydrogen should react with the air surrounding the test fixture, causing no change in the oxygen content on the airside of the YSZ plate. This assumption is supported by the fact that variation of the cathode airflow rate from 100 to 300 sccm resulted in minimal change (a couple of minivolts) in OCV. The results in Fig. 4 clearly showed low OCVs were obtained, indicating

the leak paths through mica seals were two-way, i.e., air into the fuel side and fuel into the airside, even though the fuel side was maintained slightly higher pressure than the airside. Typically, the total gas flow (or leak = L_{total}) through porous medium consists of two parts:

$$L_{\text{total}} = L_{\text{forced flow}} + L_{\text{diffusional flow}} \quad (1)$$

where $L_{\text{forced flow}}$ is the forced flow (leak) driven by a pressure gradient and $L_{\text{diffusional flow}}$ the diffusional flow (leak) driven by concentration gradients. In the two long-term OCV and cycling tests in this study, the deviations from the Nernst voltage apparently are the result of air flowing into the fuel side. Since the fuel was at a higher absolute pressure than the air, it seems appropriate to attribute the leakage to the diffusional flow of air into the fuel side driven by the oxygen concentration gradient across the seal.

3.5. Comparison of experimental leak rate with calculated leak rate from OCV tests

At 800 °C it is likely that combustion between leaked hydrogen and oxygen would occur very rapidly and reach equilibrium. As a result, the measured OCVs could be used to estimate the leak rates. The Nernst equation for open-circuit voltage of an electrochemical cell is

$$\text{OCV} = \left(\frac{RT}{nF}\right) \ln\left[\frac{P_{\text{O}_2,\text{ cathode}}}{P_{\text{O}_2,\text{ anode}}}\right] \quad (2)$$

where R is the ideal gas constant, T the absolute temperature, n the number of electrons associated with the electrochemical reaction, F the Faraday constant, and P_{O_2} the equilibrium oxygen partial pressure at the cathode or the anode side. From measured OCVs, one can calculate the equilibrium P_{O_2} at the anode side assuming the equilibrium oxygen partial pressure at cathode side is constant (P_{O_2} = 0.21). And from $P_{\text{O}_2,\text{anode side}}$, one can estimate the initial (transient) oxygen concentration ($C(\text{O}_2)_{\text{transient oxygen}}$) at the anode side, based on possible chemical reactions between the following gases: H_2, O_2, H_2O, CO, CO_2 and OH. From estimated transient oxygen concentration in the fuel stream at the anode side, the leak rate ($L_{\text{air leak}}$) can be calculated by

$$L_{\text{air leak}} = \frac{Q_{\text{fuel+air leak}} C(\text{O}_2)_{\text{transient oxygen}}}{C(\text{O}_2)_{\text{air}}} \quad (3)$$

where $C(\text{O}_2)_{\text{air}}$ (=0.21) is the oxygen concentration in air and $Q_{\text{fuel + air leak}}$ the total gas flow rate of the fuel and the leaked air, but was assumed to be constant of initial fuel stream (63 sccm) since the air leak rate by diffusion process was expected to be small. Using OCV = 0.920 V and the equations mentioned, we can estimate the air leak rates for hybrid mica (sample #1, pressed at 100 psi at cycle #671) to be 0.66 sccm, or 0.032 sccm cm^{-1} when normalized with the outer leak length of the 2 in. × 2 in. test fixture.

Leak rates were also measured directly. The 800 °C leak rate of sample #1 at thermal cycle #671 was measured with ultra-high-purity helium initially set at 2 psig within the sealed anode chamber through external tubing. The details of the leak test and the rate determination are given elsewhere [8]. By monitoring the pressure drop with time, one can calculate the leak rates through the mica seals. Fig. 5A shows the pressure versus time of the leak test of sample #1 at cycle #671. Fig. 5B shows the slope (leak rate) of Fig. 5A versus helium pressure. The leak rate at a differential pressure of ~0.2 psi was ~0.018 sccm cm^{-1} at 800 °C. This experimentally measured leak rate for helium with a 0.2 psi differential across the seal (~0.018 sccm cm^{-1}) was similar to, but somewhat lower than, the leak rate for oxygen in air calculated from OCV values (~0.032 sccm cm^{-1}).

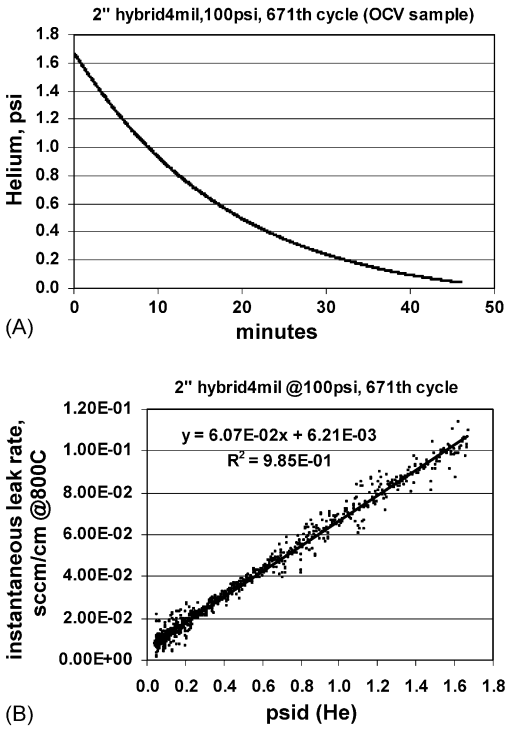

Fig. 5. Leak test of sample #1 at thermal cycle #671. (A) The actual pressure vs. time data and (B) the slope (leak rate) of (A) vs. the helium pressure in psid (i.e., pressure difference between the helium and the surrounding air).

4. Summary and conclusions

We have conducted long-term thermal cycle tests of two 2 in. × 2 in. hybrid Phlogopite mica-based seals. OCV was measured during thermal cycles to assess the stability of these compressive mica seals. Both mica samples showed the desired thermal cycle stability with minimum drop of OCV over as many as 1000 cycles. Leak rates calculated from the measured OCV also showed good agreement with direct leak rate measurements. Overall, the hybrid Phlogopite mica seal has demonstrated the desired thermal cycle stability for solid oxide fuel cells in a simulated SOFC environment.

Acknowledgements

The authors would like to thank S. Carlson for SEM sample preparation, and J. Coleman for SEM analysis. This paper was funded as part of the Solid-State Energy Conversion Alliance (SECA) Core Technology Program by the US Department of Energy's National Energy Technology Laboratory (NETL). Pacific Northwest National Laboratory is operated by Battelle Memorial Institute for the US Department of Energy under Contract No. DE-AC06-76RLO 1830.

References

[1] T. Yamamoto, H. Itoh, M. Mori, N. Mori, T. Watanabe, Compatibility of mica glass-ceramics as gas-sealing materials for SOFC, Denki Kagaku 64 (6) (1996) 575–581.
[2] K. Ley, M. Krumpelt, J. Meiser, I. Bloom, J. Mater. Res. 11 (1996) 1489.
[3] N. Lahl, D. Bahadur, K. Singh, L. Singheiser, K. Hilpert, J. Electrochem. Soc. 149 (5) (2002) A607–A614.
[4] S.B. Sohn, S.Y. Choi, G.H. Kim, H.S. Song, G.D. Kim, J. Non-Cryst. Solids 297 (2) (2002) 103–112.
[5] S. Tanaguchi, M. Kadowaki, T. Yasuo, Y. Akiyamu, Y. Miyaki, K. Nishio, J. Power Sources 90 (2000) 163–169.
[6] K.S. Weil, J.S. Hardy, J.Y. Kim, Use of a novel ceramic-to-metal braze for joining in high temperature electrochemical devices, in: Joining of Advanced and Specialty Materials, vol. 5, American Society of Metals, 2002, pp. 47–55.
[7] K.S. Weil, J.S. Hardy, J.Y. Kim, Development of a silver–copper oxide braze for joining metallic and ceramic components in electrochemical devices, in: Proceedings of the International Brazing and Soldering 2003 Conference, American Welding Society, 2003.
[8] Y.-S. Chou, J.W. Stevenson, L.A. Chick, Ultra-low leak rate of hybrid compressive mica seals for solid oxide fuel cells, J. Power Sources 112 (1) (2002) 130–136.
[9] S.P. Simner, J.W. Stevenson, Compressive mica seals for SOFC applications, J. Power Sources 102 (12) (2001) 310–316.
[10] Y.-S. Chou, J.W. Stevenson, Mid-term stability of novel mica-based compressive seals for solid oxide fuel cells, J. Power Sources 115 (2) (2003) 274–278.
[11] Y.-S. Chou, J.W. Stevenson, Thermal cycling and degradation mechanisms of compressive mica-based seals for solid oxide fuel cells, J. Power Sources 112 (2) (2002) 376–383.
[12] Y.-S. Chou, J.W. Stevenson, Phlogopite mica-based compressive seals for solid oxide fuel cells: effect of mica thickness, J. Power Sources 124 (2) (2002) 473–478.